pISSN 1738-2696 · eISSN 2212-5469
http://dx.doi.org/10.1007/s13770-016-9048-7
ORIGINAL ARTICLE

TERM

Microfluidic Spinning of the Fibrous Alginate Scaffolds for Modulation of the Degradation Profile

Cho Hay Mun[1†], Ji-Young Hwang[1†], Sang-Hoon Lee[1,2,3*]

[1]Department of Biomedical Engineering, College of Health Science, Korea University, Seoul, Korea
[2]Department of Bio-convergence Engineering, College of Health Science, Korea University, Seoul, Korea
[3]KU-KIST Graduate School of Converging Sciences & Technology, Korea University, Seoul, Korea

In tissue engineering, alginate has been an attractive material due to its biocompatibility and ability to form hydrogels, unless its uncontrollable degradation could be an undesirable feature. Here, we developed a simple and easy method to tune the degradation profile of the fibrous alginate scaffolds by the microfluidic wet spinning techniques, according with the use of isopropyl alcohol for dense packing of alginate chains in the microfiber production and the increase of crosslinking with Ca^{2+} ion. The degradation profiling was analyzed by mass losses, swelling ratios, and also observation of the morphologic changes. The results demonstrated that high packing density might be provided by self-aggregation of polymer chains through high dipole interactions between sheath and core fluids and that the increase of crosslinking rates could make degradation of alginate scaffold controllable. We suggest that the tunable degradation of the alginate fibrous scaffolds may expand its utilities for biomedical applications such as drug delivery, *in vitro* cell culture, wound healing, tissue engineering and regenerative medicine.
Tissue Eng Regen Med 2016;13(2):140-148

Key Words: Alginate; Degradation; Isopropyl alcohol; Cross-linking; Microfluidic spinning

INTRODUCTION

Recent progress in tissue engineering and regenerative medicine has enabled generation of diverse bioengineered tissue substitutes for replacement or improvement of tissues or organs [1]. Scaffold design and fabrication are prior to tissue regeneration and biomaterial applications [2,3]. Since engineering of tissue or organ substitutes preferentially requires the extracellular matrix (ECM) that can closely mimic *in vivo* environment for cell-biomaterial interactions and cell adhesion, ECM-like scaffold materials have been developed, including alginate, collagen, chitosan, gelatin, silk, synthetic polymers, etc. [4-9]

Alginate is one of the best ECM candidate biomaterials, for it is nontoxic, biodegradable, and easily available from natural sources. This has been widely useful in the food, cosmetics, and pharmaceutical industries due to its outstanding chemical and physical properties. Moreover, alginate has recently been used in regeneration of skin, cartilage, bone, liver, and islet [9-13]. The rapid gelling properties of alginate enable the simple and cost-effective production of microstructures with spherical, fibrous, or tubular shapes using microfluidic devices. These structures may be effectively used to form three-dimensional (3D) scaffolds that may play a critical role in cell adhesion, cell growth, and new tissue formation [4,5]. Fibrous 3D scaffolds can modulate porosity and microtopology of a scaffold, permitting easy transport of nutrients, gases, and wastes, and also guide the direction and growth of cells.

Although fibrous alginate scaffolds take some advantages, it has proven to be difficult to modulate their degradation properties, thereby it is posing a critical barrier to the extensive application of alginates. The degradability of alginate has been regulated by a variety of methods, including photocrosslinking, intermolecular covalent crosslinking with glutaraldehyde, or blends of alginate with synthetic polymers such as poly (lactide-co-glycolide) (PLGA) [5,14-16]. Photocrosslinking reactions typically involve the use of a light sensitizer or the release of an acid, which may be harmful to the body or cells and also exposure to ultraviolet light can damage encapsulated cells [17]. Calcium sulfate ($CaSO_4$) has been used as an ionic crosslinker to extend the degradation time; however, the gelation kinetics associated with $CaSO_4$ are difficult to control, and the

Received: July 6, 2015
Revised: July 26, 2015
Accepted: July 28, 2015
***Corresponding author:** Sang-Hoon Lee, Department of Biomedical Engineering, College of Health Science, Korea University, 145 Anam-ro, Seongbuk-gu, Seoul 02841, Korea.
Tel: 82-2-3290-5654, Fax: 82-2-921-6818, E-mail: dbiomed@korea.ac.kr
†These authors contributed equally to this work.

resulting structures are not uniform [4]. The controllable degradation of ionic crosslinked alginate scaffolds under *in vivo* conditions would greatly assist the development of alginate scaffold applications [18]. The degradation rate of alginate gels strongly depend on the degree of oxidation, pH, and the temperature [19].

In this paper, we described a simple and easy method for regulating the degradation profiles of the alginate microfibers. Since microfluidic spinning techniques enable the ready modulation of the physiochemical properties of a microfiber, a microfluidic chip was used to generate micro-engineered hydrogels [7,20-22]. In our system, the alginate chains were packed in the fiber through a low-polarity sheath flow, as isopropyl alcohol (IPA) was used to maximize the packing density of this polymer [23,24] and the degree of crosslinking with calcium ions was increased by extending curing time of the alginate fibers in an ionic crosslinking solution. We hypothesized that aligned dense packing of alginate chains in the microfibers and a high degree of crosslinking of alginate with Ca^{2+} ions could slow down the degradation rates of alginate fibers and provide a means for controlling the degradation of the alginate scaffolds. To ensure the maintained scaffold's structure on cell culturing period, a myoblast cell line cultured on these alginate fibers enhanced cell proliferation.

MATERIALS AND METHODS

Fabrication process of the fibers by microfluidic spinning

Microfluidic chips were fabricated using an SU-8 (MicroChem, Westborough, MA, USA) photoresist-patterned silicon wafer as a mold. The polydimethylsiloxane (PDMS) pre-polymer and cross-linker (Sylgard 184, Dow Corning, Midland, MI, USA) were mixed in a 10:1 ratio, poured onto the mold, and cured at 80°C for 2 hours. The PDMS substrates were then bonded together using oxygen plasma treatment. The prepared devices were heated in an oven at 80°C for 1 day to recover the hydrophobic surface properties [25,26]. The effects of the calcium chloride ($CaCl_2$, Sigma, St. Louis, MO, USA) concentration and IPA (Sigma, St. Louis, MO, USA) sheath flow on the degradation were investigated by fabricating under the four conditions: two different sheath solutions with 3% w/v $CaCl_2$ in distilled water (DW) or IPA and two different curing times for 1 hr or 12 hrs. A schematic diagram of the alginate fiber generation process is illustrated in Figure 1.

Characterization of the alginate fibers

For characterization of the surface properties of each alginate fiber, attenuated total reflectance Fourier transform infrared (ATR-FTIR) spectroscopy was performed, equipped with a Universal ATR diamond accessory of Perkin Elmer Spectrum 100 (PerkinElmer, Waltham, MA, USA). Transmission and ATR spectra were recorded with 10 scans at a resolution of 4 cm^{-1} between 4000 and 800 cm^{-1}.

In order to investigate the crystallinity of each fiber structure, X-ray diffraction (XRD) measurements were performed on a D/max-2500 X-ray diffractometer (Rigaku, Tokyo, Japan) equipped with a Cu kα source. The one-dimensional XRD patterns with the intensity curves and a function of 2θ, the scattering angle, were obtained from integration of the two-dimensional scattering patterns of each sample.

Inductively coupled plasma-optical emission spectroscopy (ICP-OES; PerkinElmer, Waltham, MA, USA) analysis revealed the amount of Ca^{2+} ions involved in cross-linking the fibers. The degree of crosslinking for the fibers prepared with a 1 h curing time was compared to that obtained after a 12 hrs curing time. Each fiber sample was washed thoroughly with water and ethanol and then dried for 1 day at room temperature (RT). An equal mass (0.8 g) of each sample was used in the subsequent analysis.

Analysis of the degradation rate

To investigate the degradation rates, each alginate fiber generated from each condition was soaked with 5 mL of culture media containing Dulbecco's modified Eagle's medium (DMEM), 10% fatal bovine serum and 1% penicillin/streptomycin (Life Technologies, Carlsbad, CA, USA) in a 6 well plate and then incubated in a humidified incubator at 37°C with 5% CO_2. At the end points of fixed time, the remained fiber samples were replaced from the culture media, washed thoroughly with DW, and dried at RT overnight in a laminar flow hood, followed by measuring the weights of the degraded or swollen scaffolds in use of a precision weighing balance (Mettler Toledo, Columbus, OH, USA). The degradation rates were assessed by calculating the weight loss (%) and the swelling ratio (%).

Weight loss was defined using the following expression:

$$\text{Weight loss (\%)} = [(W_i - W_d)/W_i] \times 100,$$

where W_i=initial weight and W_d=weight after degradation. Here, W_i and W_d are the weights of the fibers before and after degradation, respectively.

The dried alginate fibers were immersed into the culture medium at 37°C. The weights of the swollen samples were measured after the excess surface solution had been removed on a filter paper. The swelling ratio was calculated using the following expression:

$$\text{Swelling ratio (\%)} = [(W_t - W_0)/W_0] \times 100,$$

where W_t=weight of the swollen fibrous scaffold and W_0=weight of the dried fibrous scaffold after incubation for a period of time.

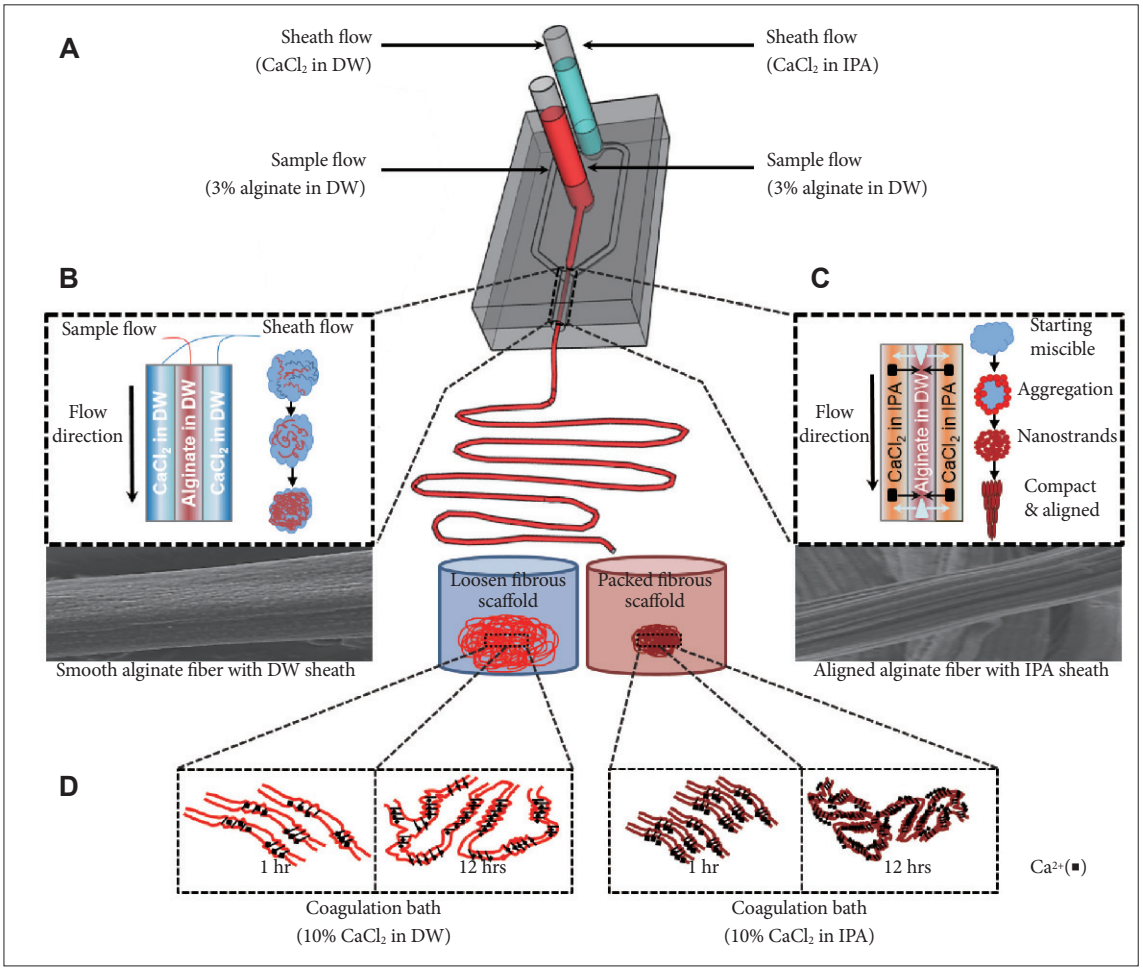

Figure 1. Schematic diagram of the microfluidic system for alginate fiber fabrication. (A) Illustration of a PDMS microfluidic chip, consisted of the inlet and outlet channels. Alginate solution was used as sample fluid, while calcium chloride was used for sheath fluids with distilled water (DW) or IPA. (B) General fiber fabrication process and (C) dehydration process applied to the aqueous alginate fibers in an IPA solvent via chemical focusing. (D) The gelation process of the alginate fibers in DW or in IPA solution according to each time point, mediated by the cross-linking of alginate chains with Ca^{2+} ions. PDMS: polydimethylsiloxane, IPA: isopropyl alcohol.

Observations of the morphologic changes

The effects of dehydration by IPA were examined by observing the morphologic changes on the fiber surfaces using scanning electron microscopy (SEM, JEOL JSM-5600LV, Tokyo, Japan). After the samples were dehydrated using graded ethanol series from 25%, 50%, 75%, 95% to 100%, the fibers were dried at RT overnight. The samples were mounted on a specimen stub using carbon paste, coated with palladium alloy, and observed at an acceleration of 10 kV.

Assays of cell proliferation and cell viability

The functionality of the alginate fibers as scaffolds was investigated using a mouse myoblast cell line, C2C12 (American Type Culture Collection, Manassas, VA, USA). The cells were cultured in culture media in a humidified 5% CO_2 environment at 37°C and maintained in subconfluent state prior to the experiments. The media was changed to prevent myoblast differentiation. For initial adhesion and proliferation experiments, the cells were seeded at about 5×10^4 cells/200 μL onto the alginate fibrous scaffolds, which had been coated with type I collagen (Sigma-Aldrich, St. Louis, MO, USA).

Cell proliferation was measured on day 0, 1, 3, 5, and 7 using the cell counting kit-8 (CCK-8; Dojindo Molecular Technologies, Kumamoto, Japan) according to the manufacturer's instructions. The absorbance of each sample was read at 450 nm using a microplate reader (SpectraMax M2, Molecular Devices, Sunnyvale, CA, USA). The viability of cells was also evaluated by incubating cells using Live/Dead assay reagents (50 mM calcein-AM and 25 mg/mL ethidium homodimer-1; Invitrogen, Carlsbad, CA, USA) in culture medium for 40 min at 37°C. The labeled cells were subsequently observed and the images were acquired by a confocal microscopy (Olympus, Tokyo, Japan).

Statistical analysis

All experiments in the study were repeated at least three times. The mean±standard deviation are reported here. The significance of the differences between groups was evaluated using a two-tailed Student's t-test. Levels of $p<0.05$ and $p<0.01$ were considered to be statistically significant.

RESULTS

Fabrication of the calcium alginate fiber scaffolds

By microfluidic wet spinning technique and immersion method in coagulating solution, the alginate fibers were fabricated. To control the degradation rates, we alternated the contents of flow solutions and curing time in the coagulation bath; sheath solutions containing either 3% $CaCl_2$ in DW or in IPA and coagulation time for either 1 hr or 12 hrs in 10% $CaCl_2$. Since the sample fluids with 3% (w/v) alginate and the sheath fluids with 3% (w/v) $CaCl_2$ solution either in DW or in IPA were used, solidification of the alginate solution was occurred at different interfaces between two liquids (Fig. 1A).

Highly negative charged alginate molecules are strongly crosslinked with positive charged calcium ions. The calcium solution with DW in sheath flow slowly passes through the alginate solution in the sample flow, so that the alginate fibers are generated with the smooth, round surfaces (Fig. 1B). On the other hand, IPA in sheath flow greatly affects the fiber structure with compact, contracted and aligned forms, when IPA permeates the surfaces of alginate solution, gets quickly aggregated and forms nanostrands (Fig. 1C). After the fabrication process, those fibers were immersed in a coagulation bath for 1 hr or 12 hrs and then four types of the calcium alginate fibers were successfully fabricated (Fig. 1D). Characterization and the degradation rates of each fiber were further analyzed.

Characterization of the surfaces on the alginate fibers

Figure 2A demonstrates the FTIR spectra of calcium alginate fibers in water (blue line) and in IPA (red line). There are two comparable characteristic groups; one is the stretching vibration bands of -OH group centered at near 3300 cm^{-1} and the other is the stretching bands of COO-group at near 1580 cm^{-1} (asymmetric) and 1410 cm^{-1} (symmetric). The broad and smooth band of hydroxy group in IPA-based alginate fibers has shifted to lower wavenumbers, because of the strong ionic interactions between calcium ions and the OH groups or the rearrangement of intra-molecular hydrogen bonds in the surface of alginate fibers. The OH band of the IPA-based fibers at 3240 cm^{-1} was broad and smooth, with a shift to lower wavenumbers, although the peak did not show a strong intensity [27]. This broad feature has been attributed to the ionic interactions between ions and the OH groups or the formation of intra-molecular hydrogen bonds [28]. The observed shift was mainly due to the rearrangement of hydrogen bonds. The spectra of carboxylate ion in calcium alginate fibers with IPA was observed at 1578 cm^{-1} and 1405 cm^{-1}, and those with water at 1586 cm^{-1} and 1418 cm^{-1}, the asymmetrical and the symmetrical stretching of carboxyl groups, respectively. These shifts in IPA to lower wavenumbers might indicate an interaction of the tight structure in the intermolecular chains of alginate fibers with the calcium ions in comparison with water-based alginate fibers.

Figure 2B shows one-dimensional XRD patterns of the calcium alginate fibers from water-based (blue line) and IPA-based (red line) sheath fluids. Both patterns are similar, as the peaks in both groups were observed at $2\theta=23.80°$ in the spectra. The strengths of the 2θ patterns in the spectra reflected the degree of crystallinity. IPA-based alginate fibers provide little sharper and stronger diffraction peaks, which indicate higher crystallinity and a more perfect ordering, compared to the fibers fabricated with the water-based sheath flow.

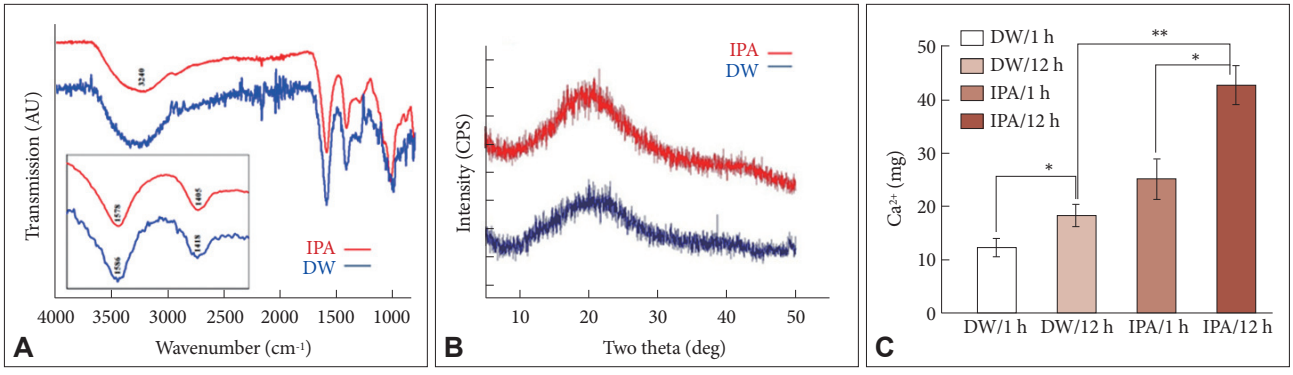

Figure 2. Characterization of the alginate fibers formed using different core and sheath flow conditions. (A) ATR-FTIR analysis and (B) XRD patterns of the alginate fibers prepared from water-based (blue line) and IPA-based $CaCl_2$ sheath solutions (red line). (C) Analysis of calcium ion concentration by ICP-OES in each fiber, indicated with the blue boxes for water-based $CaCl_2$ sheath solutions and the red boxes for IPA-based $CaCl_2$ sheath solutions (*$p<0.05$ and **$p<0.01$). ATR-FTIR: attenuated total reflectance Fourier transform infrared, XRD: X-ray diffraction, ICP-OES: inductively coupled plasma-optical emission spectroscopy, IPA: isopropyl alcohol.

The Ca^{2+} ion concentrations in the alginate fibers

The amounts of Ca^{2+} incorporated into each fiber, as determined using ICP-OES, are showed in Figure 2C. The curing times for the alginate fibers, which mediated the calcium ion cross-linking of the alginate chains, was governed by the diffusion coefficient of calcium in the sheath and coagulation solutions [29]. The ICP-OES results revealed that the amount of Ca^{2+} ions in the fibers increased as the curing time in the $CaCl_2$ coagulation bath increased. A curing time increase from 1 to 12 hrs increased the amount of Ca^{2+} incorporated into ionic crosslinks from 12.5±2.1 mg (1.0-fold) to 18.3±2.6 mg (1.46-fold), while curing times of 1 or 12 hrs in a sheath solution with IPA yielded Ca^{2+} ion contents that were 25.2±4.1 mg (2.02-fold) and 43.5±3.8 mg (3.48-fold increases), respectively.

The degradation rates of the alginate fibers

Figure 3 shows the weight losses and swelling ratios of the alginate fibers prepared from various curing times, as determined to the degradability of each fiber after soaking in a DMEM cell culture medium at 37°C. The mass loss over time was determined according to the degradation (Fig. 3A). The alginate fibrous scaffold prepared in a DW sheath with 1 hr curing time displayed the fastest degradation with mass loss of 92.7±2.8% within 7 days. As the curing time increased from 1 hr to 12 hrs, the mass loss decreased to 39.8±2.5% for the fibers in DW sheath flow. The mass loss was 37.5±2.1% for the fibers in IPA with the curing time for 1 hr, while that in IPA sheath flow with 12 hrs curing displayed the slowest degradation with 19.7±4.9% mass loss for 7 days.

The swelling ratios of the each type of alginate fibers in culture medium are shown in Figure 3B. The alginate fibrous scaffolds prepared in DW sheath fluid displayed rapid swelling and this swelling ratios increased up to 3 days and then gradually decreased, whereas the swelling of the alginate in IPA sheath fluid slowly increased. The changes of the swelling ratios from each alginate fibrous scaffold measured over time reflected the changes in the physical and chemical structures of the fibers. The amounts of Ca^{2+} presence in the alginate fibrous scaffold was correlated with the swelling ratio after 7 days. These results showed that the networks decreased in weights through the degradation process and the weight loss and swelling ratio were found to be highly correlated.

Morphologic changes according to the degradation rates

The SEM images for morphology observations shown in Figure 4 revealed the same profiling of degradability that corresponded to the weight losses and the swelling ratios. The fiber sizes of the fibrous alginate scaffold prepared in a DW sheath with 1 hr curing time were 9.47±1.46 μm. Whereas the curing time increased from 1 hr to 12 hrs, the diameter of the fibers decreased to 8.72±0.41 μm for the fibers. The size was 5.32±0.47 μm for the fibers in IPA with the curing time for 1 hr, while that in IPA sheath flow with 12 hrs curing displayed the slightly decreased sizes with 5.28±0.22 μm. These results indicate that IPA treatment makes the fibers more compact and longer cross-linking has little effects on the compact sizes.

While the alginate fibers from DW sheath fluid have the smooth surfaces (Fig. 4A and B), aligned fiber structures formed in the IPA sheath fluid as a result of self-aggregation (Fig. 4C and D). Figure 4E-H show that the surfaces of the alginate fibers changed dramatically on day 7 after incubation with cul-

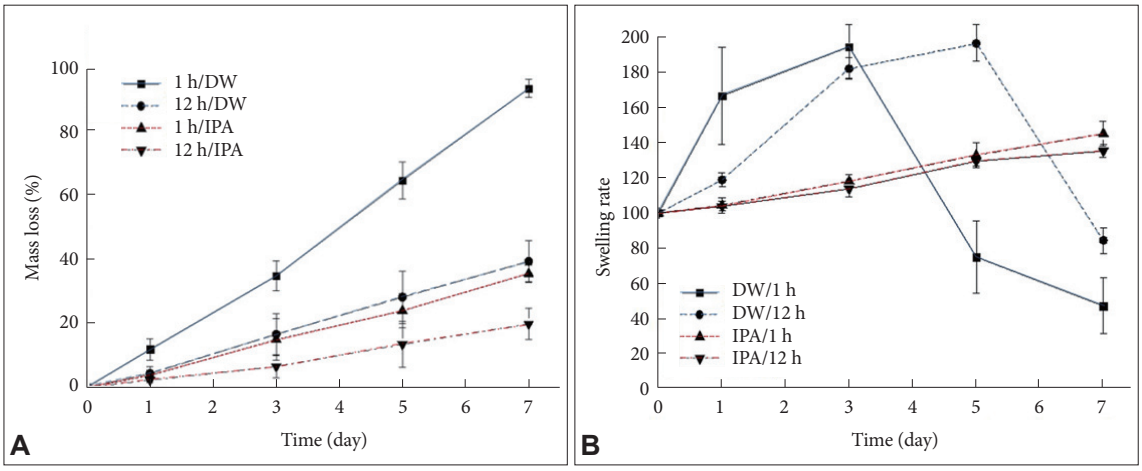

Figure 3. Degradation and the swelling ratios of the alginate fibers. Time-dependent (A) mass loss and (B) swelling ratio of four types of fibers. The alginate fibers prepared from water-based $CaCl_2$ sheath solutions indicate with the blue lines and that from IPA-based $CaCl_2$ solutions with the red lines. The values represent the means and standard deviations (N=4). DW: distilled water, IPA: isopropyl alcohol.

ture medium on the alginate fibrous scaffolds and that longer fiber curing time for 12 hrs produced strong, distinct fiber structures. Supplementary Figure 1 (in the online-only Data Supplement) shows more detailed SEM images of alginate fibers immersed in DMEM without cells on the day 7.

On the contrary, Supplementary Figure 2 (in the online-only Data Supplement) shows that alginate fibers had a smoother looser morphology after the fibers were cultured with myoblast C2C12 cells seeded and cultured in the DMEM culture medium and the cells were removed by trypsin at 7 days. The surfaces of the alginate fibers cultured with cells were more mottled than the fiber surfaces incubated without cells. Polymer scaffolds such as alginate have been shown to degrade in acidic environments through surface erosion [30]. The diameters of the alginate fibers obtained from the images followed the same trend as the swelling ratio (Fig. 3B). A comparison data on the alginate fibrous scaffolds with or without cells demonstrated that the scaffolds prepared without cells (Supplementary Fig. 1 vs. Supplementary Fig. 2) were degraded to a lesser degree than the scaffolds that had been incubated with cells for 7 days.

The cell viability and proliferation on the alginate fibers

To investigate the cell viability and proliferation, CCK-8 assay was carried out after seeding myoblast C2C12 cells onto the alginate fibrous scaffolds. The result data as normalized versus the value obtained on day 0. Figure 5A shows that the percentile of viable cells that attached and grew were higher on the alginate fibers prepared with the IPA sheath fluid than those with the DW sheath fluid. The proliferation of the C2C12 cells also increased with the curing time within fibers prepared using a given sheath fluid. The number of survived cells on the scaffolds increased was changed from DW to IPA as the sheath fluid because the alginate fibrous scaffolds prepared with the IPA degraded less than those with the DW sheath fluid. Figure 5B-E show that live, immnuostained C2C12 cells on the alginate fibrous scaffolds on culture day 7, coincided with the results of the cell viability assay.

DISCUSSION

For tissue repair and regeneration, the scaffolds play an important role, so that many studies on affordable scaffold materials have been developed during past decades. Applicable scaffolds for tissue engineering should promote cell-ECM-scaffold interaction, provide controllable biodegradability, transport nutrients, gases, wastes and also drugs for cell proliferation and/or differentiation, and also lower toxicity and immune reactions to the minimum levels [31-33].

We developed an improved microfluidic wet spinning method for regulating the degradation properties of the alginate fibers by optimizing the density of the ordered alginate chain structures and by increasing the degree of crosslinking with Ca^{2+}, resulted in significantly increased cell proliferation. The polymer chains in the fibers could be densely packed through the use of a low-polarity sheath flow. In this work, a highly ordered alginate fiber was generated through dipole-dipole attractions at the dehydrating interface between the aqueous sample and IPA sheath fluids [23]. The structure of the ordered polymer chains resembled the crystalline structure of fibroin

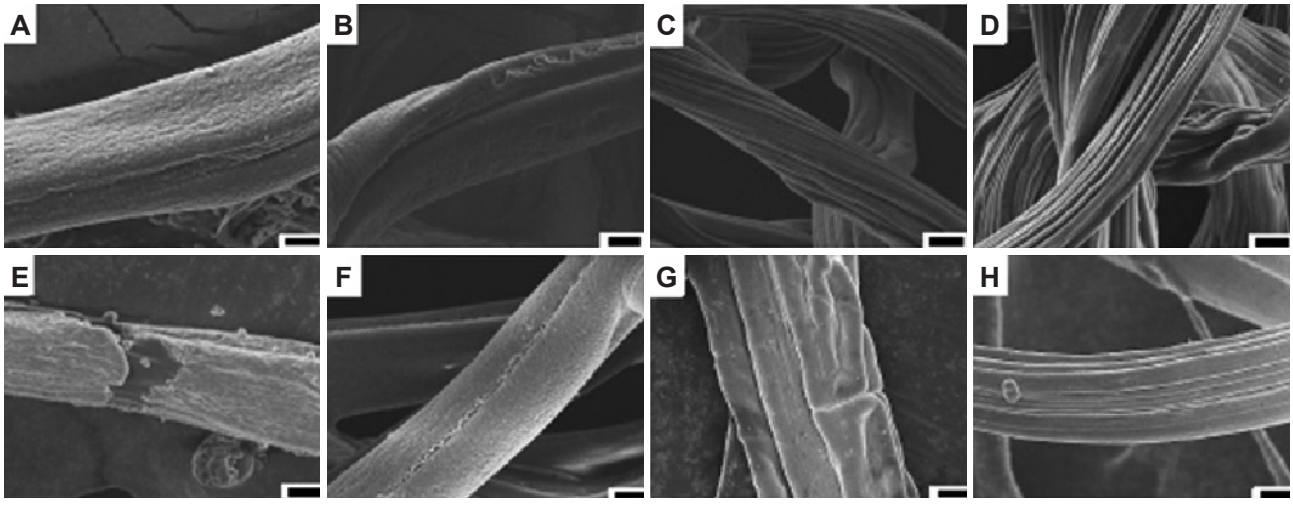

Figure 4. SEM images of the alginate fibrous scaffolds prepared from various conditions. (A-B & E-F) Alginate fibers prepared from DW- or (C-D & G-H) IPA-based sheath fluids. (A, C, E, and G) With curing conditions for 1 hr or (B, D, F, and H) 12 hrs in 10% $CaCl_2$ bath. (A-D) Before or (E-H) after immersion in culture medium for 7 days. The scale bars indicate 10 μm. SEM: scanning electron microscopy, DW: distilled water, IPA: isopropyl alcohol.

[34]. These results suggested that the solvent system induced conformational changes that produced an ordered structure through dehydration, in coincidence with the SEM data [30].

Crosslinking is an effective method of stabilizing 3D polymer networks. Several types of crosslinking agents may be utilized for different applications. In this study, we employed the ionic crosslinking with divalent cations, which is commonly used to prepare alginate hydrogels. An increase in crosslinked calcium concentration can affect formation of hydrogels and proper reaction time may require to an appropriate character. Divalent cations bind to guluronate and block the alginate chains. Guluronate can block one polymer chain and form junctions with the guluronate blocks of adjacent polymer chains in what is termed the "egg-box model of cross-linking", resulting in a gel structure [35]. Calcium ions diffuse into the alginate sample solution flow and crosslink alginate within the microfluidic channel (Fig. 1B and C) [9,36,37]. The gelation time for such alginate fibers is governed by the available concentration of Ca^{2+} ions and the diffusion coefficient of calcium in the alginate solution. As the calcium chloride concentration is increased from 3% (w/v) $CaCl_2$ in the sheath solution to 10% (w/v) $CaCl_2$ in the coagulation bath, all Ca^{2+} ion binding sites in the alginate chains present at the fluid flow interface became occupied by cations during the initial moments of the gel formation process [38]. Whereas the cations rapidly bound to the polymer because all of the Ca^{2+} ion binding sites in the alginate chains were unoccupied, Ca^{2+} ions were subsequently prevented from forming additional crosslinks in the gelling zone because diffusion through the pre-formed gel surface layer was kinetically hindered. The resistance to Ca^{2+} ion diffusion into the core region of the alginate fibers suggested that the calcium ions required a longer curing time to permit full binding in the alginate fibers. The local concentration of $CaCl_2$ and the residence time were controlled to mature the gelled network [29].

The mass loss and equilibrium swelling ratios due to degradation would be affected by the solvents, crosslinking density and time. The mass loss behavior may correlate with the weight changes. That is, the weight loss would be in reciprocal proportion to the molar mass (molecular weight) loss with time. As degradation of alginate scaffolds was monitored by measuring the changes of the dry weight loss and swelling ratios with time, the conditions of increasing weight loss of alginate and decreasing crosslinking density during degradation resulted in a higher equilibrium swelling ratio.

During the initial stages of fiber degradation after preparation in the DW sheath fluid for 1 hr or 12 hrs, low degree of ion exchanges of the Ca^{2+} ions with Na^{+} ions was permitted. The Na^{+} ions did not damage the fiber network, although the lattice size was enlarged. The swelling ratio, therefore, increased during the initial period. Once the ion exchange reaction had reached a critical value, the entire crosslinking network was expected to become disjointed, resulting in the dissolution of the alginate fibers Supplementary Figure 3 (in the online-only Data Supplement). Placing the Ca^{2+} crosslinked alginate fibers in DMEM resulted in fiber degradation and swelling mainly as a result of the ion exchange process between the Ca^{2+} ions present in the egg-box cavities of the polyguluronate blocks and the Na^{+} ions in the buffer solution [39,40].

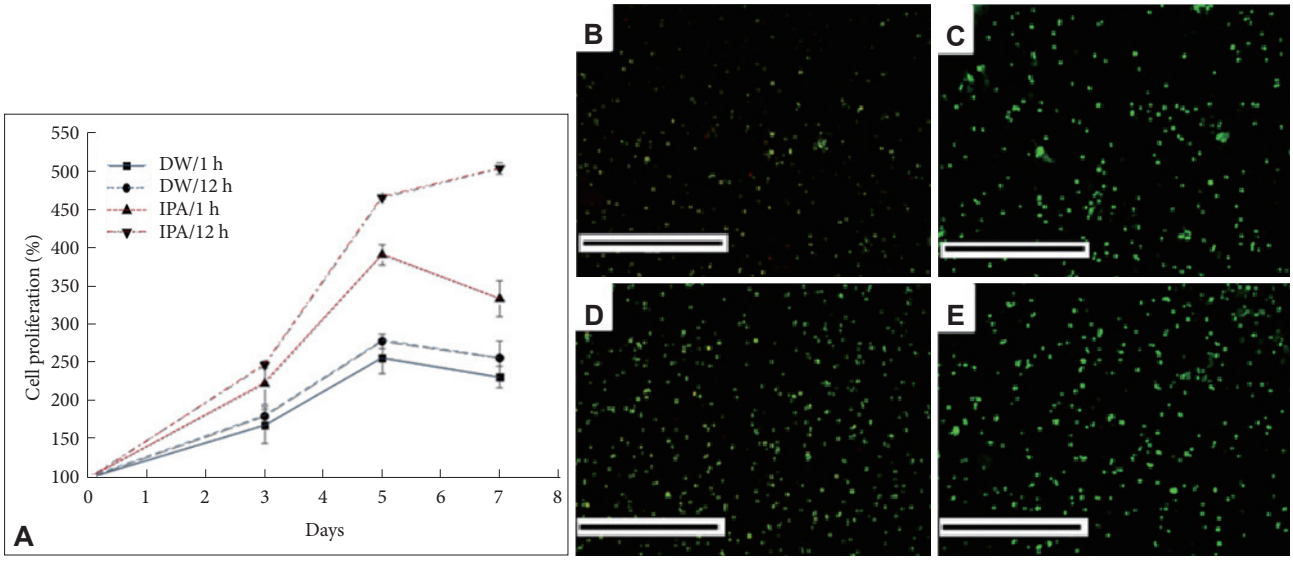

Figure 5. Cell viability assay with mouse myoblast C2C12 cells cultured on each alginate fibrous scaffold. (A) Time-dependent cell proliferation. Live & dead immunostaining images on (B) alginate fibrous scaffolds prepared from the DW sheath fluid with 1 hr or (C) 12 hrs curing and on (D) alginate scaffold from the IPA sheath fluid with 1 hr or (E) 12 hrs curing. The green fluorescence indicates the live cells at day 7. The scale bars are 1000 μm. DW: distilled water, IPA: isopropyl alcohol.

The changes in the alginate fiber swelling ratio were found to fully characterize the degradation of these alginate fibers, as the swelling ratio was strongly related to the crosslinked and self-aggregated structure. Figure 3B shows that the alginate fibers in DMEM produced large swelling ratios, and the rate of water diffusion into the samples was faster than the degradation process. After 3 days, the swelling ratio began to slow and the fiber erosion process began. These processes may limit the attachment and proliferation of cells on the calcium alginate fiber scaffolds. The swelling ratio of fibers prepared in the IPA sheath fluid with 1 hr or 12 hrs curing times increased due to the partial degradation of the alginate fibers possessing more calcium ions and a large degree of self-aggregation. SEM images of the alginate fibrous scaffolds revealed the results of bulk erosion (Supplementary Figs. 1 and 2). These results suggested that the degradation of fibrous alginate scaffolds is a bulk erosion process. The swelling ratio of each alginate fibrous scaffold differed according to the crosslinking and self-aggregation density [41].

The cell seeding efficiency and growth on the scaffold was enhanced by applying a type-I collagen coating onto the alginate fibrous scaffold. Collagen, a primary structural ECM protein, has excellent cell-binding properties and cell compatibility, making it a widely useful biomaterial in the tissue engineering field. Collagen scaffolds provide the necessary support for cells to attach, proliferate, and maintain their differentiated function. For this reason, it is important to match the rate at which the scaffold is degraded to the rate at which cells proliferate [42]. The cell proliferation assessment showed that the alginate fibrous scaffold prepared with the IPA sheath fluid and a 12 hrs curing time provided the most stable scaffold, with a slow degradation rate [43]. These results revealed that alginate exposed to IPA formed highly ordered structures with compact alignments and provided suitable micro-scaled topography with more grooved surfaces for tissue engineering, enhancing cell adhesion, proliferation or differentiation [44,45].

Microfluidic spinning methods enable control over the material composition, size, and shape, degradation rates of fibers. Thereby, these methods have been central to tissue engineering and biomedical engineering applications [46]. Here, we successfully demonstrated that the degradation properties of an alginate fibrous scaffold could be tuned according to high degree of crosslinking with Ca^{2+} ions and compactness of the self-aggregate structures formed under dipole interactions between the sheath and core fluids by IPA.

Our controlled degradable alginate scaffold may have the potential to provide optimal platform to the cells, to delivery useful factors/drugs to the cells and to serve as a good matrix for tissue engineering and regeneration.

Supplementary Materials

The online-only Data Supplement is available with this article at http://dx.doi.org/10.1007/s13770-016-9048-7.

Acknowledgements

This work was supported by National Research Foundation of Korea (NRF-2015R1A2A1A09004998), Republic of Korea.

Conflicts of Interest

The authors have no financial conflicts of interest.

Ethical Statement

There are no animal experiments carried out for this article.

REFERENCES

1. Langer R, Vacanti JP. Tissue engineering. Science 1993;260:920-926.
2. Langer R, Tirrell DA. Designing materials for biology and medicine. Nature 2004;428:487-492.
3. Fisher MB, Mauck RL. Tissue engineering and regenerative medicine: recent innovations and the transition to translation. Tissue Eng Part B Rev 2013;19:1-13.
4. Kuo CK, Ma PX. Ionically crosslinked alginate hydrogels as scaffolds for tissue engineering: part 1. Structure, gelation rate and mechanical properties. Biomaterials 2001;22:511-521.
5. Lee KY, Rowley JA, Eiselt P, Moy EM, Bouhadir KH, Mooney DJ. Controlling mechanical and swelling properties of alginate hydrogels independently by cross-linker type and cross-linking density. Macromolecules 2000;33:4291-4294.
6. Paguirigan A, Beebe DJ. Gelatin based microfluidic devices for cell culture. Lab Chip 2006;6:407-413.
7. Khademhosseini A, Langer R. Microengineered hydrogels for tissue engineering. Biomaterials 2007;28:5087-5092.
8. Geckil H, Xu F, Zhang X, Moon S, Demirci U. Engineering hydrogels as extracellular matrix mimics. Nanomedicine (Lond) 2010;5:469-484.
9. Lee BR, Hwang JW, Choi YY, Wong SF, Hwang YH, Lee DY, et al. In situ formation and collagen-alginate composite encapsulation of pancreatic islet spheroids. Biomaterials 2012;33:837-845.
10. Lee BR, Lee KH, Kang E, Kim DS, Lee SH. Microfluidic wet spinning of chitosan-alginate microfibers and encapsulation of HepG2 cells in fibers. Biomicrofluidics 2011;5:22208.
11. Jun Y, Kang AR, Lee JS, Jeong GS, Ju J, Lee DY, et al. 3D co-culturing model of primary pancreatic islets and hepatocytes in hybrid spheroid to overcome pancreatic cell shortage. Biomaterials 2013;34:3784-3794.
12. Barnett SE, Varley SJ. The effects of calcium alginate on wound healing. Ann R Coll Surg Engl 1987;69:153-155.
13. Lee KH, Shin SJ, Kim CB, Kim JK, Cho YW, Chung BG, et al. Microfluidic synthesis of pure chitosan microfibers for bio-artificial liver chip. Lab Chip 2010;10:1328-1334.
14. Jeon O, Bouhadir KH, Mansour JM, Alsberg E. Photocrosslinked alginate hydrogels with tunable biodegradation rates and mechanical properties. Biomaterials 2009;30:2724-2734.
15. Ashton RS, Banerjee A, Punyani S, Schaffer DV, Kane RS. Scaffolds based on degradable alginate hydrogels and poly(lactide-co-glycolide) microspheres for stem cell culture. Biomaterials 2007;28:5518-5525.
16. Abdi SIH, Choi JY, Lau HC, Lim JO. Controlled release of oxygen from PLGA-alginate layered matrix and its in vitro characterization on the viability of muscle cells under hypoxic environment. Tissue Eng Regen Med 2013;10:131-138.

17. Lee KY, Mooney DJ. Alginate: properties and biomedical applications. Prog Polym Sci 2012;37:106-126.
18. Doyle JW, Roth TP, Smith RM, Li YQ, Dunn RM. Effects of calcium alginate on cellular wound healing processes modeled in vitro. J Biomed Mater Res 1996;32:561-568.
19. Bouhadir KH, Lee KY, Alsberg E, Damm KL, Anderson KW, Mooney DJ. Degradation of partially oxidized alginate and its potential application for tissue engineering. Biotechnol Prog 2001;17:945-950.
20. Shin Y, Han S, Jeon JS, Yamamoto K, Zervantonakis IK, Sudo R, et al. Microfluidic assay for simultaneous culture of multiple cell types on surfaces or within hydrogels. Nat Protoc 2012;7:1247-1259.
21. Andersson H, van den Berg A. Microfabrication and microfluidics for tissue engineering: state of the art and future opportunities. Lab Chip 2004;4:98-103.
22. El-Ali J, Sorger PK, Jensen KF. Cells on chips. Nature 2006;442:403-411.
23. Chae SK, Kang E, Khademhosseini A, Lee SH. Micro/nanometer-scale fiber with highly ordered structures by mimicking the spinning process of silkworm. Adv Mater 2013;25:3071-3078.
24. Ahn SY, Mun CH, Lee SH. Microfluidic spinning of fibrous alginate carrier having highly enhanced drug loading capability and delayed release profile. RSC Adv 2015;5:15172-15181.
25. Shin SJ, Park JY, Lee JY, Park H, Park YD, Lee KB, et al. "On the fly" continuous generation of alginate fibers using a microfluidic device. Langmuir 2007;23:9104-9108.
26. Hwang CM, Khademhosseini A, Park Y, Sun K, Lee SH. Microfluidic chip-based fabrication of PLGA microfiber scaffolds for tissue engineering. Langmuir 2008;24:6845-6851.
27. Oh SY, Yoo DI, Shin Y, Kim HC, Kim HY, Chung YS, et al. Crystalline structure analysis of cellulose treated with sodium hydroxide and carbon dioxide by means of X-ray diffraction and FTIR spectroscopy. Carbohydr Res 2005;340:2376-2391.
28. Yuno-Ohta N, Yamada M, Inomata M, Konagai H, Kataoka T. Gluten gel and film properties in the presence of cysteine and sodium alginate. J Food Sci 2009;74:E285-E290.
29. Hong JS, Shin SJ, Lee SH, Wong E, Cooper-White J. Spherical and cylindrical microencapsulation of living cells using microfluidic devices. Korea-Aust Rheol J 2007;19:157-164.
30. Zhang ZM, Wan MX, Wei Y. Highly crystalline polyaniline nanostructures doped with dicarhoxylic acids. Adv Funct Mater 2006;16:1100-1104.
31. Kim JH, Noh H, Kang JH, Lee BS, Choi J, Park K, et al. Characteristics of PLLA films blended with PEG block copolymers as additives for biodegradable polymer stents. Biomed Eng Lett 2011;1:42-48.
32. Dhandayuthapani B, Yoshida Y, Maekawa T, Kumar DS. Polymeric scaffolds in tissue engineering application: a review. Int J Polym Sci 2011 [Epub]. http://dx.doi.org/10.1155/2011/290602.
33. Ghim JH, Hussein KH, Park KM, Woo HM. Hepatic cell encapsulation using a decellularized liver scaffold. Biomed Eng Lett 2015;5:58-64.
34. Shasteen C, Choy YB. Controlling degradation rate of poly(lactic acid) for its biomedical applications. Biomed Eng Lett 2011;1:163-167.
35. Andersen T, Melvik JE, Gåserød O, Alsberg E, Christensen BE. Ionically gelled alginate foams: physical properties controlled by type, amount and source of gelling ions. Carbohydr Polym 2014;99:249-256.
36. Grant GT, Morris ER, Rees DA, Smith PJC, Thom D. Biological interactions between polysaccharides and divalent cations: the egg-box model. FEBS Lett 1973;32:195-198.
37. Morris ER, Powell DA, Gidley MJ, Rees DA. Conformations and interactions of pectins. I. Polymorphism between gel and solid states of calcium polygalacturonate. J Mol Biol 1982;155:507-516.
38. Blandino A, Macías M, Cantero D. Formation of calcium alginate gel capsules: influence of sodium alginate and CaCl2 concentration on gelation kinetics. J Biosci Bioeng 1999;88:686-689.
39. Bajpai SK, Sharma S. Investigation of swelling/degradation behaviour of alginate beads crosslinked with Ca2+ and Ba2+ ions. React Funct Polym 2004;59:129-140.
40. Pasparakis G, Bouropoulos N. Swelling studies and in vitro release of verapamil from calcium alginate and calcium alginate-chitosan beads. Int J Pharm 2006;323:34-42.
41. Mason MN, Metters AT, Bowman CN, Anseth KS. Predicting controlled-release behavior of degradable PLA-b-PEG-b-PLA hydrogels. Macromolecules 2001;34:4630-4635.
42. Lu L, Peter SJ, Lyman MD, Lai HL, Leite SM, Tamada JA, et al. In vitro and in vivo degradation of porous poly(DL-lactic-co-glycolic acid) foams. Biomaterials 2000;21:1837-1845.
43. Chae SK, Mun CH, Noh DY, Kang E, Lee SH. Simple fabrication method for a porous poly(vinyl alcohol) matrix by multisolvent mixtures for an air-exposed model of the lung epithelial system. Langmuir 2014;30:12107-12113.
44. Kang E, Jeong GS, Choi YY, Lee KH, Khademhosseini A, Lee SH. Digitally tunable physicochemical coding of material composition and topography in continuous microfibres. Nat Mater 2011;10:877-883.
45. Jeong GS, Lee SH. Microfluidic spinning of grooved microfiber for guided neuronal cell culture using surface tension mediated grooved round channel. Tissue Eng Regen Med 2014;11:291-296.
46. Jun Y, Kang E, Chae S, Lee SH. Microfluidic spinning of micro- and nano-scale fibers for tissue engineering. Lab Chip 2014;14:2145-2160.